Physics of AGN
Relativistic Jets

Heino Falcke
MPIfR Bonn

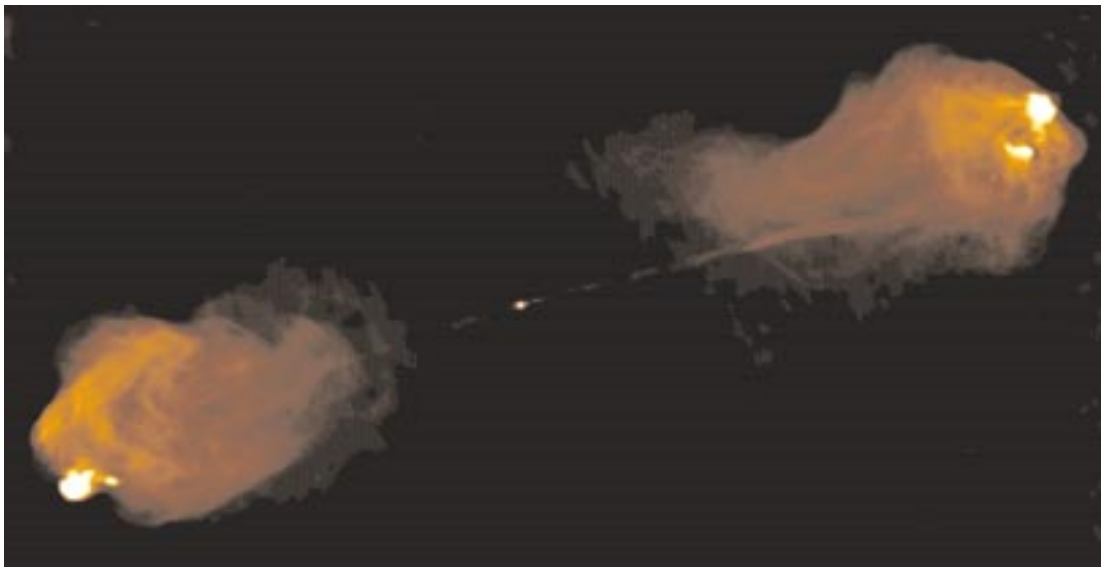

Contents:

- Relativistic Boosting
- Superluminal Motion
- Jet Kinematics
- Radio Cores

Literature:
"An Introduction to Active Galactic Nuclei", Bradley M. Peterson, Cambridge University Press, Cambridge
"Active Galactic Nuclei", Ian Robson, John Wiley & Sons, Chichester
"Radiative Processes in Astrophysics", G.B. Rybicki & A.P. Lightman, John Wiley & Sons, New York

Relativistic Jets

■ Speed of Jets

What is the speed of radio jets in AGN? Since this is non-thermal plasma where no spectral lines are seen, the Doppler-shift cannot be used to derive a jet velocity for the nucleus!

However, if the jet speed is relativistic, i.e. $v \simeq c$, relativistic effects can become important.

■ Relativistic Doppler Effect

Assume an emitting source moving at a speed $v \lesssim c$ at an angle θ with respect to the observer.
Time-dilation tells us that δt in the observers rest frame for a periodic signal with frequency ω' in the co-moving (primed) frame is

$$\nu = \frac{1}{\Delta t} = \frac{1}{\gamma \Delta t'} = \frac{\Delta \nu'}{\gamma}$$

$$\gamma = \sqrt{1 - \frac{v^2}{c^2}}$$

However, since the emitting source is moving almost as fast as the emitted photon, the source will be catching up on the photon, and travel a distance $s = v \Delta t \cos\theta$. The time difference in the arrival time of the two photons will therefore be reduced by s/c, i.e.

$$\Delta t_{\rm A} = \Delta t \left(1 - \frac{v}{c} \cos\theta\right)$$

and the observed frequency is

$$\nu = \frac{1}{\Delta t_{\rm A}} = \frac{\nu'}{\gamma \left(1 - \frac{v}{c} \cos\theta\right)}$$

This is the relativistic Doppler effect which defines the Doppler factor

$$\mathcal{D} = \frac{1}{\gamma \left(1 - \frac{v}{c} \cos\theta\right)} = \frac{\sqrt{1 - \beta^2}}{1 - \beta \cos\theta}$$

(the difference to the classical Doppler factor is only the γ factor)

Relativistic Jets

■ Relativistic Boosting

The Doppler factor is a strong function of the aspect angle and can become very large for $v \to c$.

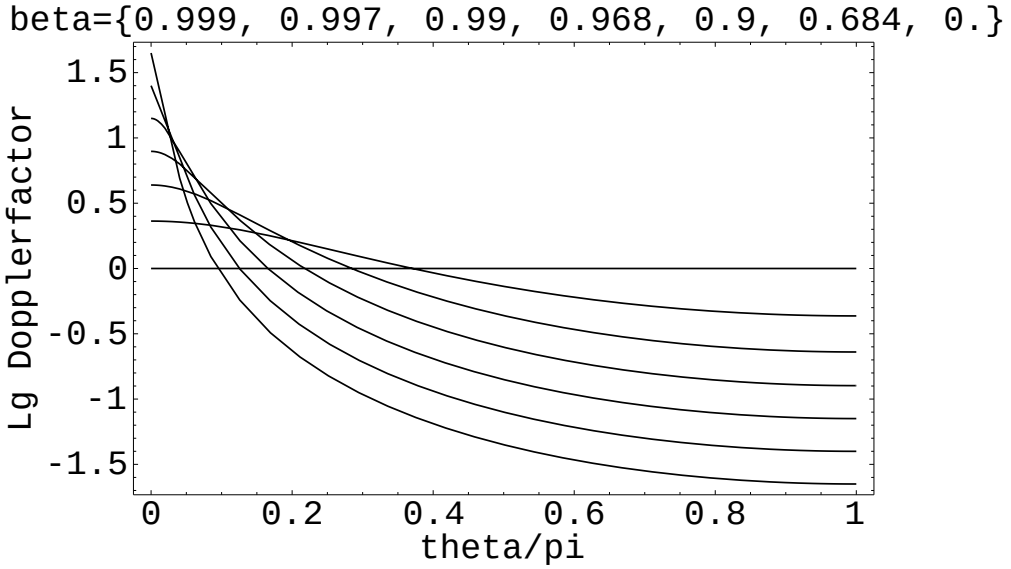

One can show (i.e. Rybicki & Lightman, chap. 4.9) that the ratio of the flux density S_ν and the frequency cubed.

$$\frac{S_\nu}{\nu^3}$$

is invariant under Lorentz transformation.

Since the observed frequency is $\nu = \mathcal{D}\nu'$ we find that also the observed flux has to be (S'_ν = flux density in co-moving frame)

$$S_\nu = \mathcal{D}^3 S'_\nu$$

Even for relatively modest relativistic velocities of $0.97c$ ($\gamma \simeq 4$), for example, the flux in the forward direction can be boosted by a factor 1000, while it is reduced by a factor 1000 in the backward direction!

Note: This effect will be reduced to $\mathcal{D}^2$ when emission from a steady jet is considered rather than from a single blob. However, since boosting will also increase the observed frequency ($\nu = \mathcal{D}\nu'$) the spectral index α ($S_\nu \propto \nu^\alpha$) of the radio spectrum will also enter in the equation, i.e. making it $\mathcal{D}^{2-\alpha}$ ($0.3 \gtrsim \alpha \gtrsim -1$).

Relativistic Jets

■ Boosting Cone

The angular effect of Doppler boosting is best shown in a polar radiation diagram for a blob moving with speed β.

```
beta={0.9, 0.874, 0.842, 0.8, 0.749, 0.684, 0.602, 0.499, 0.369, 0.206, 0.}
```

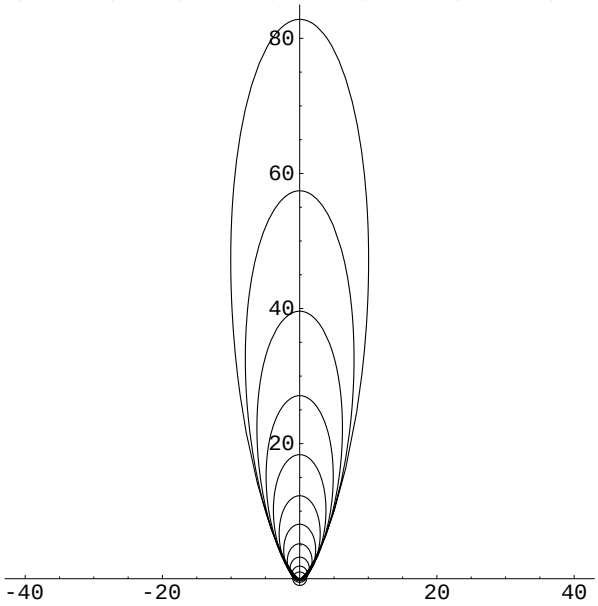

The transformation from a spherical to an elliptical polar diagram shows that angles are also transformed by relativistic effects. The so-called relativistic aberration (see Rybicki & Lightman, chap. 4.1) is given by:

$$\tan\theta = \frac{\sin\theta'}{\gamma(\cos\theta' + \beta)}$$

In the rest frame of the source, half of the radiation will be emitted from $-\pi/2$ to $\pi/2$, hence setting $\theta' = \pi/2$ will give

$$\tan\theta = \frac{1}{\gamma\beta},$$

thus for $\gamma \gg 1$ half of the radiation will be emitted in a cone with half-opening angle

$$\theta \simeq \frac{1}{\gamma}$$

Relativistic Jets

■ Jet-sidedness

Since we expect jets to be two-sided, we always have two angles under which the emission is seen by an observer: θ and $\theta + \pi$. We can now calculate the flux ratio R between jet and counter-jet under the assumption of intrinsically symmetric jets:

$$R = \frac{\mathcal{D}^2(\beta, \theta)}{\mathcal{D}^2(\beta, \theta + \pi)} = \left(\frac{1 + \beta \cos\theta}{1 - \beta \cos\theta}\right)^{2-\alpha}$$

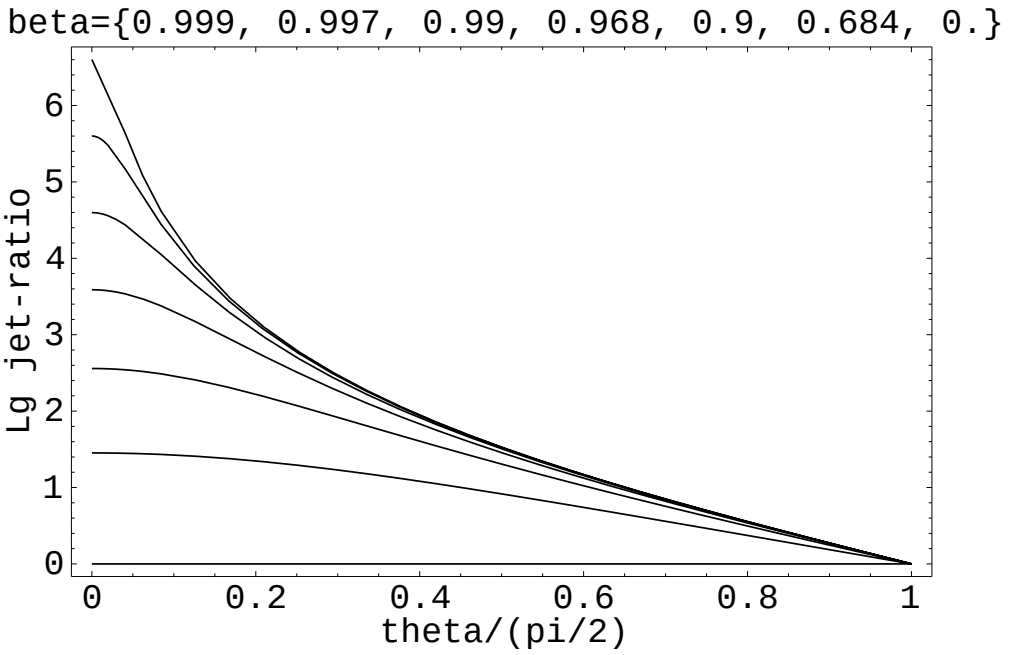

Even for mildly relativistic jets one side will always be significantly brighter than the other

This is confirmed by observations: most jets we see are one-sided.

- *pc-scale:* Most of the strong, compact radio cores seem to come from sources where the angle to the line of sight is small, these jets are always one-sided.
- *pc-scale:* Even most of the large scale jets appear to be one-sided, even though 2 extended lobes are seen indicating that really two jets are present.

Relativistic Jets

■ Jet-sidedness

For the nearby FR I radio galaxy and LINER galaxy M87 no counter-jet has been found to a limit of $R > 10^5$! Yet, there are active hotspots on both sides.

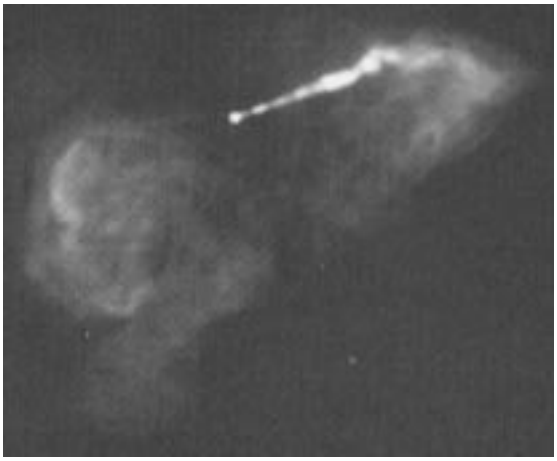

For this source angles to the line-of-sight around $30 - 50°$ and $\gamma = 3 - 6$ have been discussed. The observed R parameter therefore requires a relatively fast jet still at the kpc scale. HST observations of this jet have found proper motions that confirm relativistic speeds of $\gamma \sim 5$. Still the effect may not be strong enough to explain such a large jet-to-counterjet ratio.

Laing-Garrington Effect: Another confirmation of the boosting/orientation hypothesis comes from the Laing-Garrington Effect—the lobes on the jet-side usually show a lower rotation-measure than those on the non-jet side. This is explained by Faraday rotation of the polarized emission of the lobe on the counter-jet-side (where the jet is fainter due to boosting) by plasma in and around the galaxy.

Rotation Measure (RM): When polarized radiation moves through a hot magnetized medium (i.e. ISM) the polarization vector gets rotated. For a homogeneous medium the angle of rotation is proportional to the distance traveled within this medium.

■ Optical-Radio Correlation

Assuming that the optical/UV luminosity of quasars is 'relatively' isotropic and reflects the true engine power, one can plot the **radio core** luminosity of quasars versus UV-luminosity and see the effects of relativistic boosting.

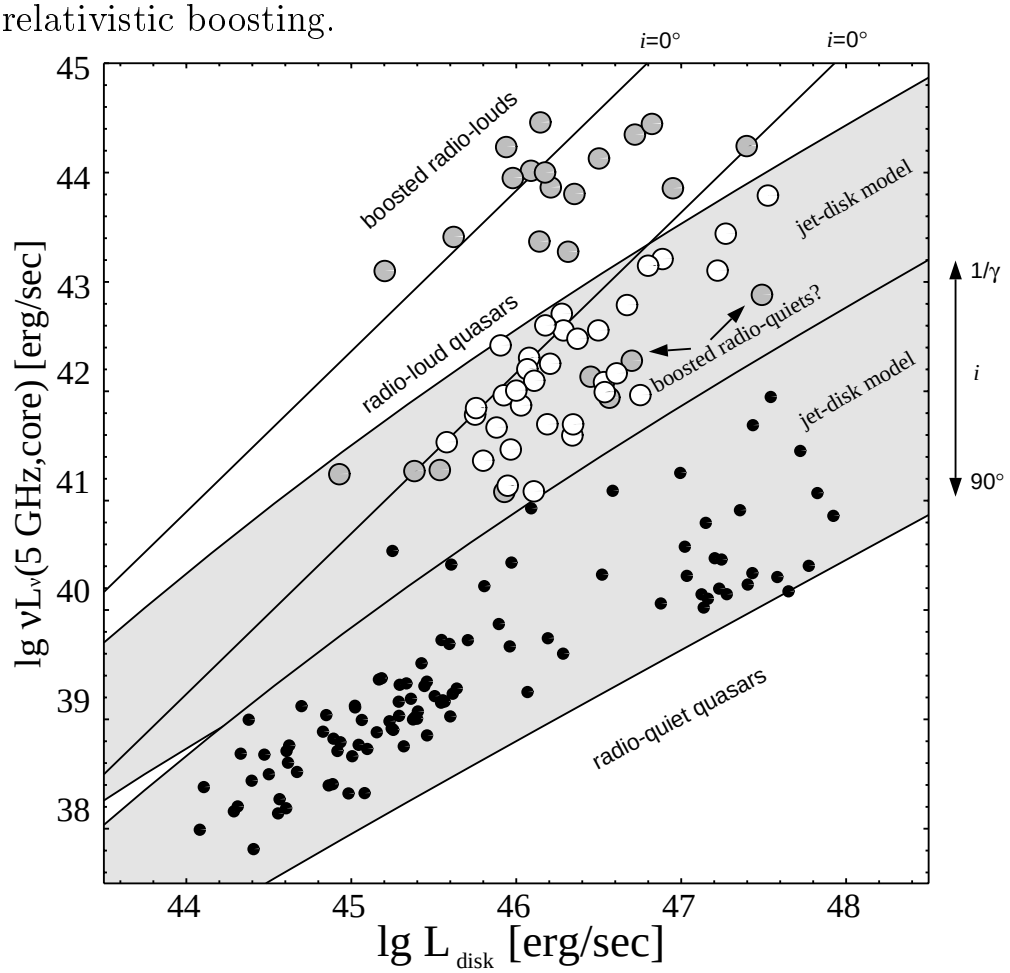

(Updated from Falcke, Malkan, & Biermann 1995)

In this plot big, white circles are radio loud, steep-spectrum quasars with FR II morphology; big, gray circles are flat-spectrum, variable, core dominated quasars (blazars). The lines represent a model where the jet power scales with optical (accretion disk) luminosity plus boosting ($\gamma \sim 3 - 10$) and random orientation. Blazars cluster at higher radio powers compared to steep-spectrum quasars. This is simply explained by small inclination angles.

Relativistic Jets

■ Brightness Temperature

The emitted flux from a black-body only depends on its temperature and size (and of course observed frequency). Hence, if one observes for a source a certain flux and size one can calculate a "virtual" temperature of the source which a black body would need to have in order to produce the observed flux. This "virtual" temperature is called "Brightness Temperature" and for a spherical source is

$$T_{\rm b} = \frac{1}{\pi r^2}\frac{c^2 S_\nu}{2k_{\rm B}\nu^2} = 1.8\cdot 10^{12}\,{\rm K}\,\left(\frac{S_\nu}{\rm Jy}\right)\left(\frac{\nu}{\rm GHz}\right)^{-2}\left(\frac{FWHM}{\rm mas}\right)^{-2}$$

Brightness temperatures which significantly exceed 10^{10}K are definitively no-longer thermal since $k_{\rm B}T > m_{\rm e}c^2$.

The brightness temperature has a very strong upper-limit for non-thermal, synchrotron radiation—the **Compton limit**. One can show (Rybicki & Lightman, chap. 7.2) that the radiation from synchrotron emission and from inverse-Compton scattering is

$$\frac{P_{\rm synch}}{P_{\rm compt}} = \frac{U_{\rm B}}{U_{\rm ph}}$$

Increasing the brightness-temperature of a source means also increasing the photon energy density $U_{\rm ph}$ (more flux in the same volume). When $U_{\rm ph} > U_{\rm B}$ ($U_{\rm B}$=magnetic field energy density) the relativistic electrons will scatter their own synchrotron-photons, thus increasing the photon energy density further. This is a run-away process, called the Compton catastrophe. The process will very quickly cool the plasma to a situation where $U_{\rm ph} \lesssim U_{\rm B}$ and hence will also limit the maximum brightness temperature of a system to

$$T_{\rm B} < 10^{12}\ {\rm K}$$

Recent space-VLBI observations (i.e. with an orbiting antenna), however, have shown that in some cores (blazars) $T_{\rm B} > 10^{12}$ K. This was actually expected since relativistic boosting will increase the flux-density without changing the size of the jet, hence it will lead to an apparent increase of $T_{\rm B}$ beyond the allowed value.

■ Apparent Superluminal Motion

A blob in a jet is initially in the core B.

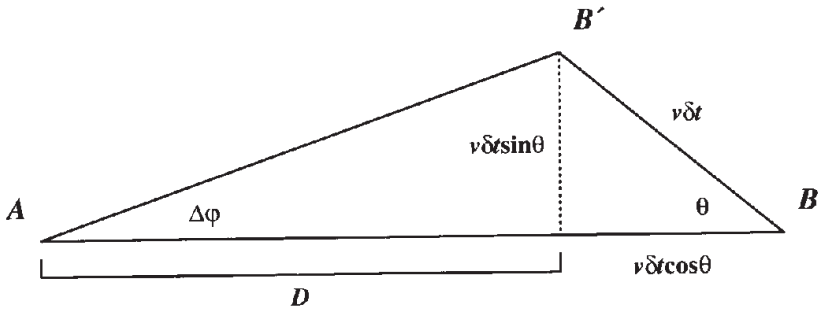

Fig. 4.6. The geometry assumed to explain apparent superluminal expansion of radio sources, i.e., where the observer at A sees a radio source move from B to B' at a speed apparently exceeding the speed of light. This effect can occur as $v \to c$ if the angle to the line of sight θ is small, but non-zero.

In the comoving frame the blob moves to position B' in the time δt — the visible angular separation between core and blob then is for an observer at A at a distance D

$$\Delta\phi = \frac{v\delta t \cos\theta}{D}.$$

Again, the blob moving at a speed close to c almost catches up on the photons and the measured time-difference it took for the blob to move from B to B' is

$$\Delta t = \delta t - \beta\delta t \cos\theta = \delta t(1 - \beta\cos\theta)$$

(no γ since the whole system is at rest with respect to the observer).

The apparent transverse velocity inferred by the observer D is therefore

$$\beta_{\rm app} = \frac{v_{\rm app}}{c} = \frac{1}{c}\frac{D\Delta\phi}{\Delta t} = \frac{1}{c}\frac{v\delta t \sin\theta}{\delta t(1 - \beta\cos\theta)} = \frac{\beta\sin\theta}{1 - \beta\cos\theta}$$

■ Apparent Superluminal Motion

The function $\beta_{\rm app} = \frac{\beta \sin\theta}{1-\beta\cos\theta}$ is a strong function of β and θ if $\beta \to 1$.

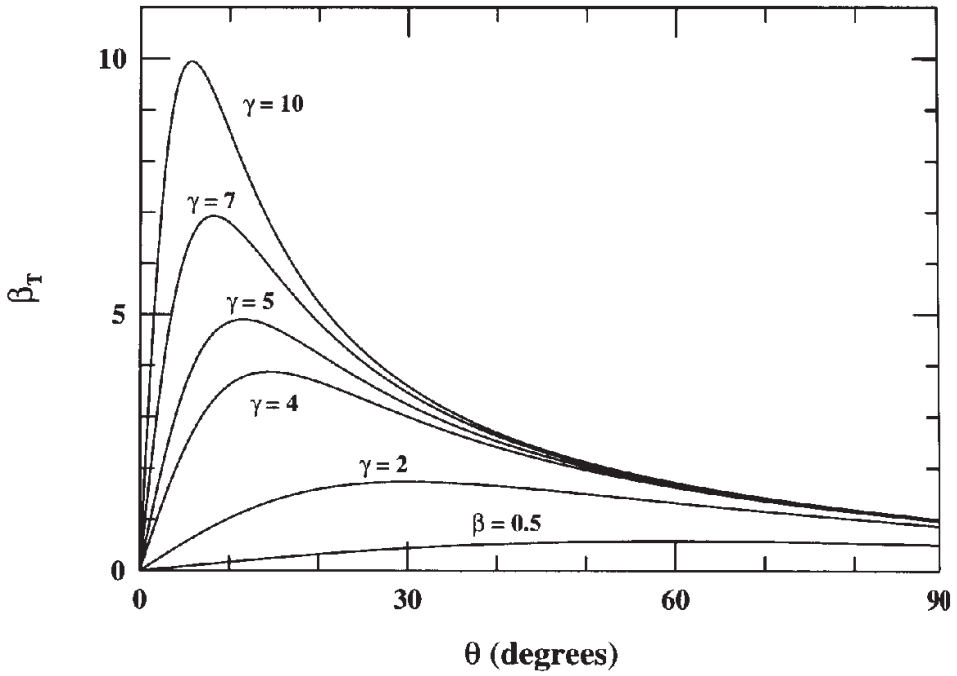

Fig. 4.7. The apparent transverse velocity $\beta_{\rm T} = v_{\rm T}/c$ of a source moving at an angle θ to the observer's line of sight (as in Fig. 4.5) as a function of the Lorentz factor $\gamma = (1-\beta^2)^{-1/2}$. For $\gamma \gg 1$, the apparent transverse velocity can exceed the speed of light.

The apparent speed is for all angles $v_{\rm app} > c$ if $\gamma \gtrsim 3$

The maximum of this function is found by solving

$$\frac{\delta\beta_{\rm app}}{\delta\theta} = 0$$

which yields $\cos\theta_{\rm max} = \beta$ and $\beta_{\rm app,max} = \beta\gamma$.

Hence, superluminal motion can be seen even for very modest γ, if the angle to the line-of-sight is small.

Note: The apparent velocity decreases again for very small angles!

■ Apparent Superluminal Motion

Such superluminal motions have been seen in many cases now and are therefore an excellent indication for the presence of relativistic speeds in the nuclei of jets.

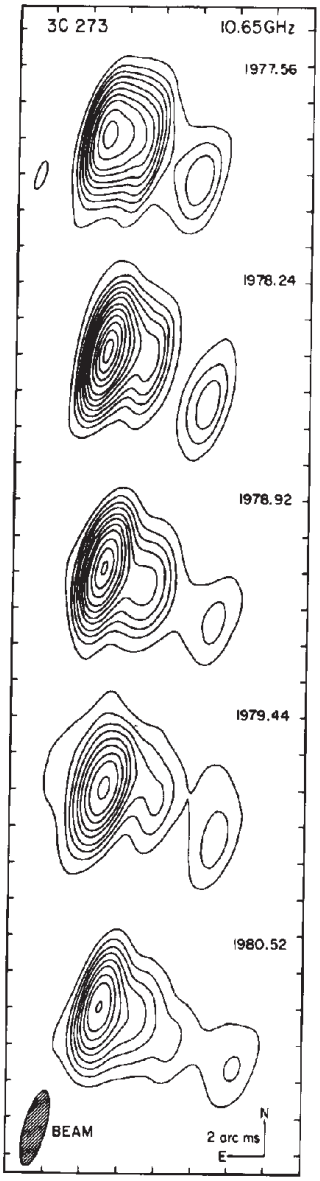

Fig. 4.5. VLBI maps at a frequency of 10.65 GHz of the quasar 3C 273 ($z = 0.158$) made at five different epochs, showing apparent 'superluminal' (i.e., faster than light) expansion of the source (from Pearson *et al.* 1981). Figure courtesy of T. J. Pearson and the California Institute of Technology. Reproduced by permission from *Nature*, Vol. 290, pp. 365–367. Copyright 1981 Macmillan Journals Limited.

■ VLBI Observations of Jet Kinematics

The proper motion of individual components can be followed with VLBI over many years. A motion of 1 mas/yr at 1 Gpc corresponds to an apparent motion of 15c—typical observed values are usually in the range 1-10c.

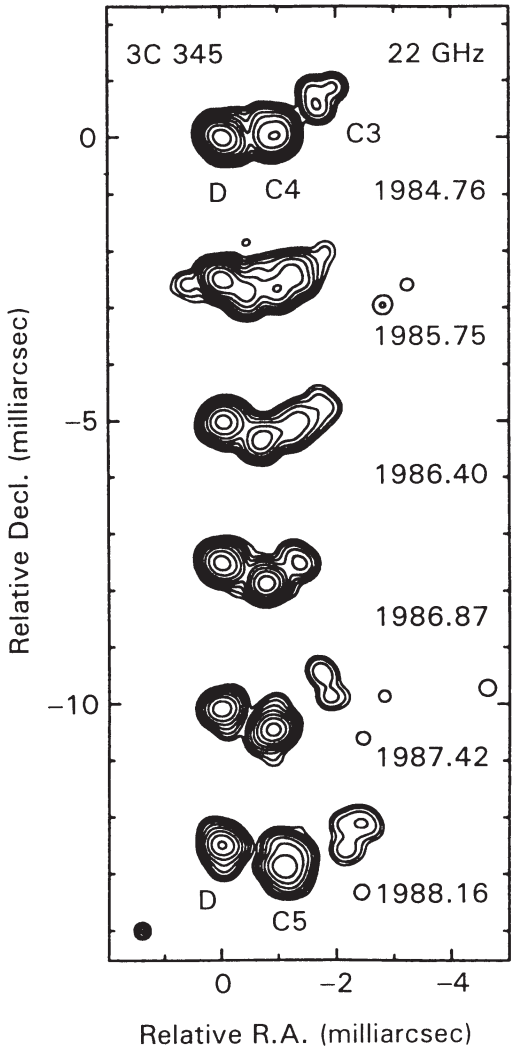

■ VLBI Observations of Jet Kinematics

One can back-interpolate the motion of individual blobs to see when they where ejected from the nucleus. An ejection of a new VLBI component is usually associated with a flare in the radio spectrum that starts at high frequencies. There are suggestions that these events are also correlated with $\gamma-$ray flares.

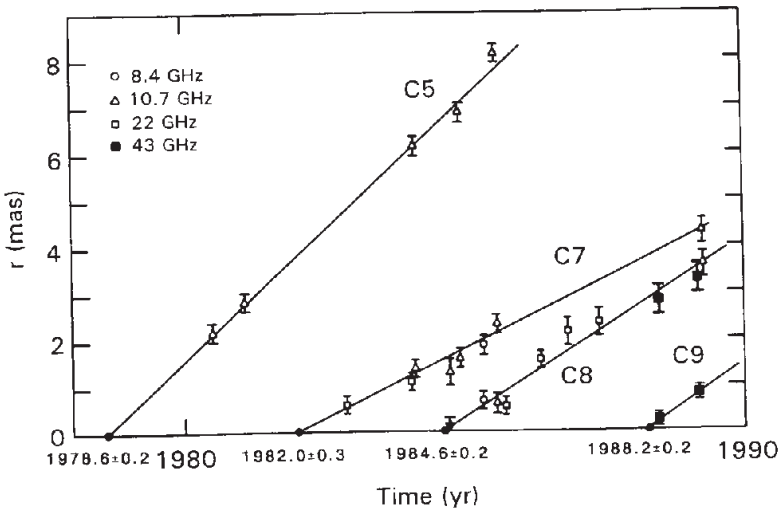

(a)

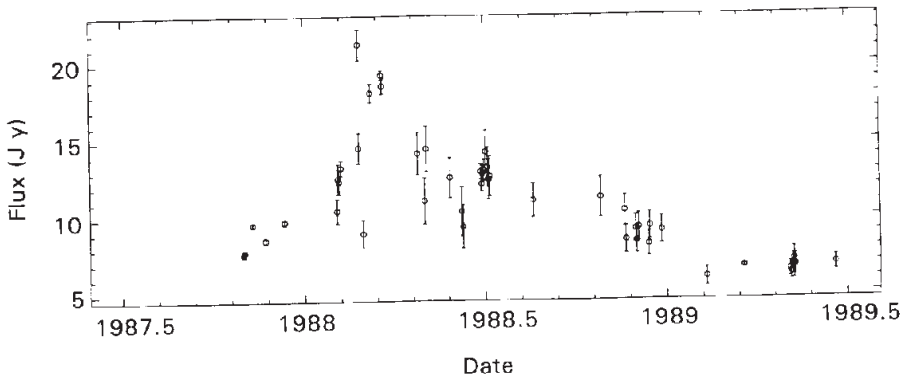

(b)

Fig. 8.6. (a) Data from millimetre VLBI of 3C273 showing the onset of a new blob and tracing it back to the time of its onset. (Krichbaum, *et al., Astron.Astrophys.*, **237**, 3, 1990.) (b) The 1.1 millimetre lightcurve showing the February 1988 flare associated with the new blob. (Robson, *et al., Mon.Not.R.Astron.Soc.*, **262**, 249, 1993.)

■ VLBI Observations of Jet Kinematics

Surprisingly, however the motion of these components are not always straight. There is clear evidence in many sources for curved trajectories.

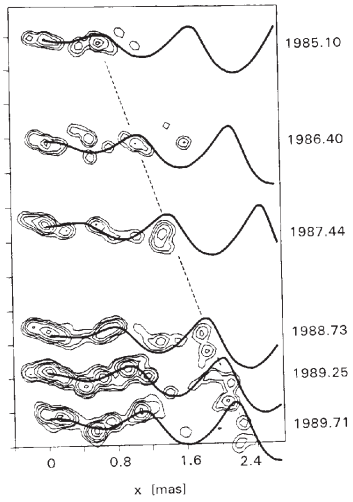

Fig. 8.5. A model of the 'sinusoidal' wiggle pattern claimed to be visible in the VLBI maps of the quasar 4C73.18. (From Roos, *et al.*, *Astrophys.J.*, **409**, 130, 1993.)

In this particular case the authors have suggested that the effect comes from a binary-black hole producing a precessing jet. After all, we know that galaxies merge and that they most likely contain central black holes. Hence, super-massive binary black holes would not be unexpected.

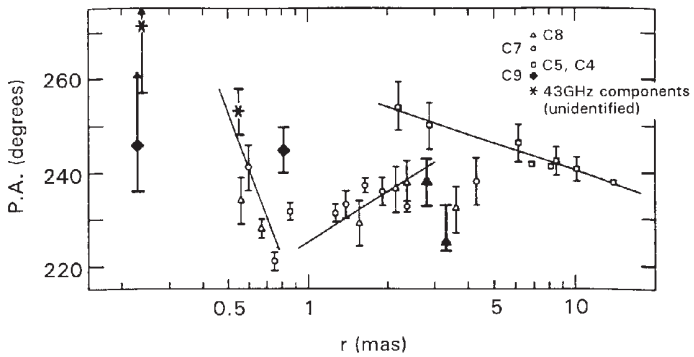

Fig. 8.4. The 'wiggle-cone' of the blobs of emission from millimetre VLBI observations of 3C273. Plotted is the position angle versus the core distance of the labelled components. (From Krichbaum, *et al.*, *Astron.Astrophys.*, **237**, 3, 1990.)

Another explanation is that blobs are just shocks on the surface of a rotating jet and not really individual blobs, producing these helical paths.

Relativistic Jets

■ Basic Jet Structure

An increased mass-ejection at the base of the jet may set up a shock in the jet flow which will propagate outwards. Such a shock could also be produced in the interface between jet and external medium. In addition to representing a local particle and energy enhancement such a shock could also lead to particle acceleration in the jet.

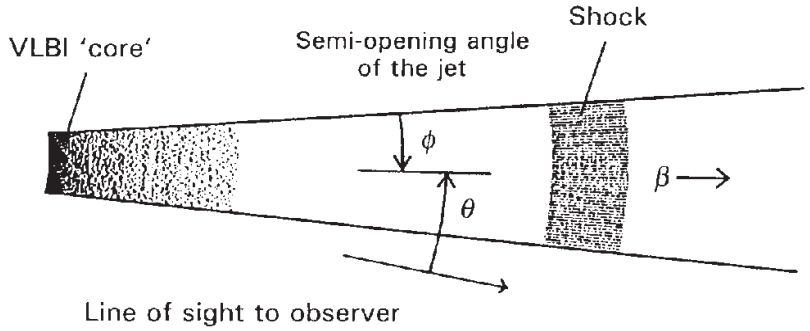

Fig. 8.9. Schematic of a shocked relativistic jet. In this picture, the flaring emission seen in the continuum synchrotron radiation along with new VLBI components originates in the shock rather than the non-shocked part of the jet.

The evolution of the spectrum of such a blob is highly non-stationary and multiple shocks and interaction regions can occur in a jet once it has left the very nucleus. The most violent shock certainly occurs at the termination shock, where the whole jet is shocked and slowed down from supersonic, relativistic to subsonic, sub-relativistic speeds. These terminal shocks (at the kpc scale) are identified with the hotspots in FR II radio galaxies and are most likely huge sites of particle acceleration.

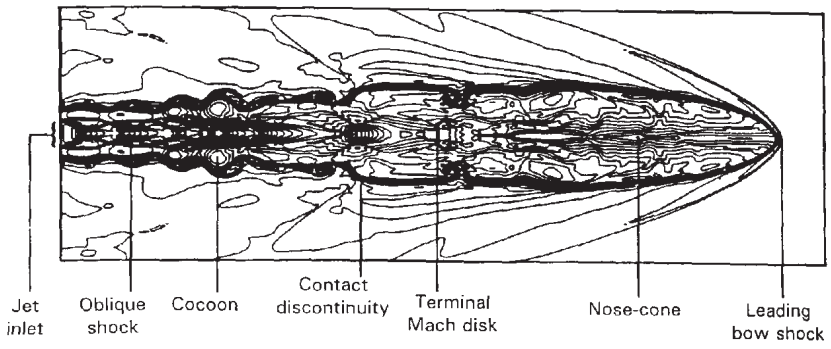

Fig. 8.3. Numerical simulation of a two-dimensional magnetically confined jet showing the relevant parameters. (From Clarke, Norman and Burns, *Astrophys.J.*, **311**, L63, 1986.)

Kompakte Radioquellen in AGN

■ Grundlagen

Wir nehmen an, daß die Energiedichte U_j des Jets bestimmt wird durch die magnetische Energiedichte U_B und die Energiedichte in relativistischen Teilchen $U_\mathrm{e+p}$. Ausserdem nehmen wir ungefähre Equipartition an, so daß

$$U_\mathrm{e+p} = kU_\mathrm{B} = kB^2/8\pi, \quad k \lesssim 1$$
$$U_\mathrm{j} = (1+k)U_\mathrm{B}$$

Die relativistischen Teilchen haben ein Potenzgesetz als Verteilungsfunktion der Form

$$\frac{dN(\gamma)}{d\gamma} = K\gamma^{-p}$$

wo wir der Einfachheit halber Protonen vernachlässigen. Dies ist bei der Berechnung er Synchrotronstrahlung im Allgemeinen gerechtfertigt, Protonen sollten aber bei der Berechnung des Energieinhaltes oder von Hochenergieemission nicht vernachlässigt werden.

Die gesamte Energiedichte in relativistischen Teilchen ergibt sich dann durch Integration über die Verteilungsfunktion

$$U_\mathrm{e+p} = K\int_{\gamma_1}^{\gamma_2} \gamma^{-p}\cdot\gamma mc^2 d\gamma \Rightarrow K = kB^2/(8\pi\Lambda m_\mathrm{e}c^2)$$

$$\lambda = \begin{cases} (\gamma_1^{2-p} - \gamma_2^{2-p})/(p-2) & \text{für } p \neq 2 \\ \ln(\gamma_2/\gamma_1) & \text{für } p = 2 \end{cases}$$

$$(\gamma_1^{2-p} - \gamma_2^{2-p})/(p-2) \propto \begin{cases} \gamma_1^{2-p} & \text{für } p > 2 \\ \gamma_2^{2-p} & \text{für } p < 2 \end{cases}$$

Mit der Wahl der Normalisierungeskonstanten können wir jetzt die Teilchendichte relativistischer Teilchen berechnen:

$$n_\mathrm{e} = K\int_{\gamma_1}^{\gamma_2} \gamma^{-p} d\gamma \simeq -K\gamma_1^{1-p}/(1-p) \quad (\gamma_2 \gg \gamma_1)$$
$$\Rightarrow n_\mathrm{e} = \frac{kB^2}{8\pi\gamma_1^{p-1}\Lambda m_\mathrm{e}c^2(p-1)}$$

Die totale Teilchendichte n ist dann gegeben durch

$$n = n_{\rm e}/x_{\rm e} \;\; x_{\rm e} \lesssim 1$$

Andererseits ist die Teilchendichte auch durch die Geschwindigkeit v, den Radius r und den Massenfluß $\dot{M}$ des Jet gegeben:

$$\dot{M}_{\rm j} = m_{\rm p} n \pi r^2 v$$

Einsetzen der obigen Gleichung ergibt dann

$$\dot{M}_{\rm j} = m_{\rm p} \pi r^2 v \frac{k B^2}{8\pi x_{\rm e} \gamma_1^{p-1} \Lambda m_{\rm e} c^2 (p-1)},$$

also kann man das Magnetfeld, ausgedrückt als Funktion der Parameter, angeben zu

$$B = \sqrt{\frac{8\pi x_{\rm e} \gamma_1^{p-1} \Lambda m_{\rm e} c^2 (p-1) \dot{M}_{\rm j}}{k m_{\rm p} \pi v}} \cdot r^{-1}$$

und für $p \neq 2$ können wir dann z.B. schreiben

$$B = 0.3\,{\rm G} \sqrt{\frac{x_{\rm e}}{\beta k} \left(\frac{p-1}{p-2}\right) \left(\frac{\gamma}{100}\right) \left(\frac{\dot{M}_{\rm j}}{M_\odot/{\rm yr}}\right)} \left(\frac{r}{\rm pc}\right)^{-1}$$

und für p=2

$$B = 0.3\,{\rm G} \sqrt{\frac{x_{\rm e}}{\beta k} \ln(\gamma_2/\gamma_1) \left(\frac{\gamma}{100}\right) \left(\frac{\dot{M}_{\rm j}}{M_\odot/{\rm yr}}\right)} \left(\frac{r}{\rm pc}\right)^{-1}$$

Kompakte Radioquellen in AGN

■ Hydrodynamik

$$P = (,\ -1)U$$

$$\rho c_{\rm s}^2 = ,\ P = ,\ (,\ -1)U$$

Für ein relativistisches Gas haben wir $,\ = 4/3$ mit der maximalen Schallgeschwindigkeit $c_{\rm s} = c\sqrt{,\ -1} = c/\sqrt{3}$ (ist erreicht, wenn die interne Energie der Elektronen größer wird als die Ruhemasse der Protonen, d.h. anfangen die Gesamtenergie zu dominieren) und somit

$$c_{\rm s} = \frac{2}{3}\sqrt{(1+k)\left(m_{\rm p}n/x_{\rm e}\right)^{-1}\frac{B^2}{8\pi}}$$

$$c_{\rm s} = \frac{2}{3}\sqrt{x_{\rm e}(1+k)\left(\frac{m_{\rm p}kB^2}{8\pi\gamma_1^{p-1}\Lambda m_{\rm e}c^2(p-1)}\right)^{-1}\frac{B^2}{8\pi}}$$

$$\Rightarrow c_{\rm s} = \frac{2}{3}\sqrt{\frac{\gamma_1 m_{\rm e}c^2}{m_{\rm p}}\left(\frac{p-1}{p-2}\right)\left(\frac{1+k}{k}\right)x_{\rm e}}$$

Die Beschränkung

$$c_{\rm s} \leq c/\sqrt{3}$$

liefert dann einen oberen Grenzwert für die minimale Elektronenenergie, bzw. Elektronenanzahl

$$\Rightarrow x_{\rm e}\gamma_1 \lesssim \left(\frac{1}{3}\right)\left(\frac{9}{4}\right)\left(\frac{m_{\rm p}}{m_{\rm e}}\right)\left(\frac{p-2}{p-1}\right)\left(\frac{k}{(1+k}\right)$$

d.h.

$$x_{\rm e}\gamma_1 \lesssim 344 \ \text{ für } p = 3 \text{ und } k \lesssim 1$$

diese Grenze kann nur signifikant überschritten werden, wenn die Equipartitionsbedingung $k < 1$ verletzt wird.
Andersherum, wenn man einen maximalen Jet haben möchte, wo $c_{\rm s} = c/\sqrt{3}$, dann muß entweder $\gamma_1 \sim 300$ oder $x_{\rm e} \sim 300$. Letzteres kann nur gehen, wenn mehr Elektronen als Protonen vorhanden sind,

also Pairs produziert werden, ersteres entspricht einem niederner-getischem Cut-Off in der Elektronenverteilung.
Energiedichte des Jets ist gegeben durch:

$$U_{\mathrm{j}} = \gamma(, U) + \gamma\rho c^2$$

und wegen $\rho c_{\mathrm{s}}^2 = , P = , (, -1)U$

$$\Rightarrow U_{\mathrm{j}} = \frac{, \rho\beta_{\mathrm{s}}^2 c^2}{, (, -1)} + \gamma\rho c^2$$

$$U_{\mathrm{j}} = \gamma\rho c^2 \left(\frac{\beta_{\mathrm{s}}^2}{, -1} + 1\right)$$

Das heißt für die maximale Schallgewschindigkeit ($c_{\mathrm{s}} = \sqrt{(, -1)}$ ergibt sich

$$U_{\mathrm{j}} = 2\gamma\rho c^2$$

(interne und Ruheenergie sind gleich)

Kompakte Radioquellen in AGN

■ Spektrum

Durch die vorangehenden Gleichungen haben wir die Teilchendichte, das Magnetfeld und den Elektron-Lorentzfaktor durch Parameter ausgedrückt und bestimmt.
Die Geometrie des Jets sei bestimmt durch freie Ausdehnung, d.h. der Jet wird sich konusförmig mit dem Öffnungswinkel seines Machkegels ausbreiten. Der halbe Öffnungswinkel ist daher

$$\sin\phi \sim \phi = \frac{1}{\mathcal{M}} = \frac{\gamma\beta}{\gamma_\mathrm{s}\beta_\mathrm{s}}$$

Der Durchmesser des Jets ist dann gegeben als Funktion der longitudinalen Koordinate

$$\Rightarrow r = \sin\phi z \sim \frac{z}{\mathcal{M}}$$

Für Teilchendichte und Magnetfeld folgt dann (aus obigen Gleichungen und letztlich aus den Erhaltunsgssätzen)

$$n \propto z^{-2} \;\;\&\;\; B \propto z^{-1}$$

Damit können wir das Spektrum des Jets ausrechnen. Die Emissivität und der Absorptionskoeffizient sind für $p = 2$ gegeben durch

$$\alpha = 4.5 \cdot 10^{-12}\mathrm{cm}^{-1}\frac{k}{\ln(\gamma_2/\gamma_1)}\left(\frac{B}{\mathrm{G}}\right)^4\left(\frac{\nu}{\mathrm{GHz}}\right)^{-3}$$

(mittlerer Pitchwinkel ist $\alpha \sim 54°$).
Kurzschreibweise:

$$\alpha = k_1 b_1^4 z^{-4}\nu^{-3}$$

$$k_1 = 4.5 \cdot 10^{-12}\mathrm{cm}^{-1}\frac{k}{\ln(\gamma_2/\gamma_1)}GHz^{-3}$$

$$k_1 = 13.9 \cdot 10^{6}\mathrm{pc}^{-1}\frac{k}{\ln(\gamma_2/\gamma_1)}GHz^{-3}$$

$$b_1 = 0.3\,\mathrm{G}\sqrt{\frac{x_\mathrm{e}\ln(\gamma_2/\gamma_1)}{\beta k}(p-1)\left(\frac{\gamma}{100}\right)\left(\frac{\dot{M}_\mathrm{j}}{M_\odot/\mathrm{yr}}\right)}$$

$$\frac{1}{\mathcal{M}} = \frac{1}{\beta\sqrt{3}}$$

Die optische Tiefe ist gegeben durch

$$\tau = 2r\alpha/\sin i$$

Damit können wir die $\tau = 1$ Fläche bestimmen:

$$1 = 2\frac{z}{\mathcal{M}}k_1 b_1^4 z^{-4}\nu^{-3}/\sin i$$

$$\Rightarrow z_{\tau=1} = \left(2\frac{1}{\sin i\mathcal{M}}k_1\right)^{1/3} b_1^{4/3}\nu^{-1}$$

$$\Rightarrow z_{\tau=1} = 50\ pc\left(\frac{1}{\beta}\frac{k_1}{13.9\cdot 10^6}\right)^{1/3}\frac{b_1}{0.3}^{4/3}\nu^{-1}$$

Note: $z_{\tau=1} \propto \nu^{-1}\dot{M}^{2/3}$ and for $\dot{M} \sim 0.03$ and $\nu = 10$ GHz $\Rightarrow z \sim 0.5$ pc. At z=0.5, d=1.5 Gpc, d.h. 0.5pc$\sim$0.5mas, das ist gerade an der Grenze von VLBI.
Die Emissivität ist

$$\epsilon = 5.5 \cdot 10^{-19}\frac{\mathrm{erg}}{\mathrm{s\,cm^3\,Hz}}\left(\frac{k}{\ln(\gamma_2/\gamma_1)}\right)\left(\frac{B}{\mathrm{G}}\right)^{3.5}\left(\frac{\nu}{\mathrm{GHz}}\right)^{-0.5}$$

$$\epsilon = k_2 b_1^{3.5} r^{-3.5}\nu^{-0.5}$$

$$k_2 = 5.5 \cdot 10^{-19}\frac{\mathrm{erg}}{\mathrm{s\,cm^3\,Hz}}\left(\frac{k}{\ln(\gamma_2/\gamma_1)}\right)GHz^{0.5}$$

$$k_2 = 1.6 \cdot 10^{37} \frac{\mathrm{erg}}{\mathrm{s\,pc^3\,Hz}} \left(\frac{k}{\ln(\gamma_2/\gamma_1)} \right) GHz^{0.5}$$

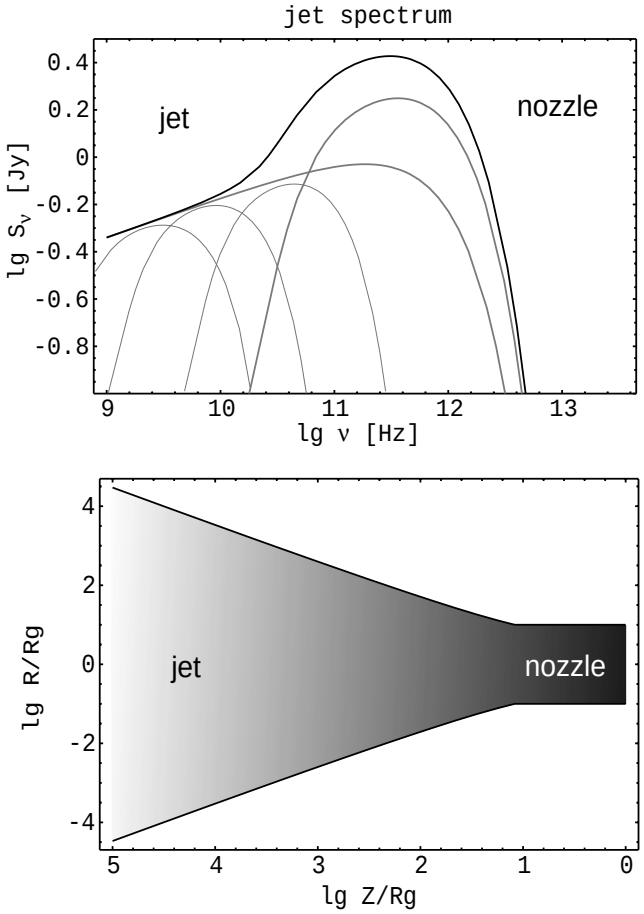

Integriere nun die Emissivität bei einer Frequenz ν in Scheiben über den gesamten Jet, beginnend bei $z_{\tau=1}$

$$L_\nu = 4\pi \int_{z_{\tau=1}}^{\infty} \epsilon(z) \pi r^2(z) / \sin(i) dz$$

$$\Rightarrow L_\nu = 4\pi^2 \mathcal{M}^{-2} \sin^{-1}(i) k_2 b_1^{3.5} \mathcal{M}^{3.5} \nu^{-0.5} \int_{z_{\tau=1}}^{\infty} z^{-3.5} z^2 dz$$

$$\Rightarrow L_\nu = 4\pi^2 \sin^{-1}(i) k_2 b_1^{3.5} \mathcal{M}^{1.5} \nu^{-0.5} z_{\tau=1}^{-0.5}$$

da aber $z_{\tau=1} \propto \nu^{-1} \Rightarrow$ ν fällt heraus und es ergibt sich ein flaches Spektrum.

Um den beobachtbaren Fluß zu erhalten, teile durch $4\pi D^2$:

$$S_\nu = 1100 Jy \left(\frac{D}{1.5\ Gpc}\right).$$

$$b_1 \propto \sqrt{\dot{M}} \quad z_{\tau=1} \propto \dot{M}^{2/3}$$

$$\Rightarrow S_\nu \propto \dot{M}^{3.5/2} \dot{M}^{-1/2 \cdot 2/3} \propto \dot{M}^{1.75-0.33} \propto \dot{M}^{1.42}$$